

Antitumor Activity of the MEK Inhibitor TAK-733 against Melanoma Cell Lines and Patient-Derived Tumor Explants

Lindsey N. Micel^{1,2}, John J. Tentler¹, Aik-Choon Tan¹, Heather M. Selby¹, Kelsey L. Brunkow¹, Kelli M. Robertson¹, S. Lindsey Davis¹, Peter J. Klauck¹, Todd M. Pitts¹, Esha Gangolli³, Robyn Fabrey⁴, Shawn M. O'Connell⁴, Patrick W. Vincent⁴, and S. Gail Eckhardt¹

Abstract

The goal of this study was to investigate the activity of the selective MEK1/2 inhibitor TAK-733 in both melanoma cell lines and patient-derived melanoma xenograft models. *In vitro* cell proliferation assays using the sulforhodamine B assay were conducted to determine TAK-733 potency and melanoma responsiveness. *In vivo* murine modeling with eleven patient-derived melanoma explants evaluated daily dosing of TAK-733 at 25 or 10 mg/kg. Immunoblotting was performed to evaluate on-target activity and downstream inhibition by TAK-733 in both *in vitro* and *in vivo* studies. TAK-733 demonstrated broad activity in most melanoma cell lines with relative resistance observed at $IC_{50} > 0.1 \mu\text{mol/L}$ *in vitro*. TAK-733 also exhibited activity in 10 out of 11 patient-derived explants with tumor growth inhibition ranging from 0% to 100% ($P < 0.001$ –0.03). Interestingly,

BRAF^{V600E} and NRAS mutational status did not correlate with responsiveness to TAK-733. Pharmacodynamically, pERK was suppressed in sensitive cell lines and tumor explants, confirming TAK-733-mediated inhibition of MEK1/2, although the demonstration of similar effects in the relatively resistant cell lines and tumor explants suggests that escape pathways are contributing to melanoma survival and proliferation. These data demonstrate that TAK-733 exhibits robust tumor growth inhibition and regression against human melanoma cell lines and patient-derived xenograft models, suggesting that further clinical development in melanoma is of scientific interest. Particularly interesting is the activity in BRAF wild-type models, where current approved therapy such as vemurafenib has been reported not to be active. *Mol Cancer Ther*; 14(2); 317–25. ©2014 AACR.

Introduction

Melanoma is the most aggressive form of skin cancer and is characterized by poor survival outcomes and limited therapeutic options. An estimated 123,590 new cases of melanoma were diagnosed in the United States in 2011, with a 5-year survival rate of advanced-stage melanoma of 15% (1). The MAPK pathways are signaling networks that transfer growth factor signals from cell surface receptors to the nucleus through protein kinase cascades. The RAS/RAF/MEK/ERK pathway is one of the best-characterized MAPK pathways and serves to transmit extracellular signals that ultimately regulate cellular

proliferation, differentiation, migration, cell-cycle, angiogenesis, and survival (2–5). In many malignancies, including melanoma, the MAPK pathway has been shown to be upregulated, either through overexpression of extracellular growth factor ligands or by constitutive activation through mutations in RAS or RAF (2, 3, 6, 7). With the upregulation of this pathway, a malignant phenotype can emerge, characterized by hyperproliferation of tumor cells, decreased apoptosis, and enhanced invasion and migration (4, 7, 8). Activating mutations in BRAF have been found in approximately 60% of primary melanoma tumors (6, 9). The most common BRAF mutation is the V600E valine to glutamic acid substitution at codon 600. This mutation leads to dysregulation and constitutive activation of the RAF/MEK/ERK pathway, resulting in abnormal cell growth and ultimately malignant transformation (4, 6–8, 10). Furthermore, it has been demonstrated that many of these tumors harboring the V600E mutation are dependent on the RAS/RAF/MEK/ERK pathway for survival and proliferation (11–14). MEK is a serine/threonine kinase that is part of the BRAF downstream signaling cascade and is responsible for the phosphorylation of ERK1/2. Interestingly, ERK1/2 appears to be the sole targets of MEK, making MEK an interesting target for anticancer therapeutics (15–18).

The development of BRAF inhibitors has provided a new treatment option for BRAF-mutated melanoma. Unfortunately, despite an impressive initial response, many patients have relapsed on BRAF inhibitor therapy. Posttreatment biopsies of resistant tumors have identified RTK, NRAS, COT, and

¹Division of Medical Oncology, University of Colorado, Anschutz Medical Campus, Aurora, Colorado. ²Division of Pediatric Hematology/Oncology, Children's Hospital Colorado, Anschutz Medical Campus, Aurora, Colorado. ³Takeda Pharmaceuticals, Inc., Cambridge, Massachusetts. ⁴Takeda Pharmaceuticals, Inc., San Diego, California.

Note: Supplementary data for this article are available at Molecular Cancer Therapeutics Online (<http://mct.aacrjournals.org/>).

Current address for L.N. Micel: Children's Hospital Colorado 4125 Briargate Parkway, #200, Colorado Springs, CO 80920.

Corresponding Author: John J. Tentler, Division of Medical Oncology, University of Colorado, 12801 E. 17th Avenue MS-8117, Aurora, CO 80045. Phone: 303-724-3887; Fax: 303-724-3879; E-mail: john.tentler@ucdenver.edu

doi: 10.1158/1535-7163.MCT-13-1012

©2014 American Association for Cancer Research.

C-RAF-mediated activation of the MEK/ERK pathway, essentially bypassing BRAF altogether (19–23). The ultimate result of MAPK pathway activation by any of the above mechanisms is MEK protein kinase activation and ERK1/2 phosphorylation with subsequent nuclear translocation and gene transcription, resulting in a proliferative and antiapoptotic, BRAF-inhibitor-resistant phenotype.

TAK-733 (Takeda California) is an investigational potent, selective, non-ATP-competitive allosteric inhibitor of MEK kinase (24, 25). In *in vitro* assays, TAK-733 inhibits MEK kinase selectively, and potently inhibits growth in a broad range of cell lines (24, 25). In mouse xenograft efficacy studies, TAK-733 has demonstrated substantial tumor growth suppression and shrinkage in a wide range of tumor types (24). As MEK inhibitors act downstream of BRAF, resistance to BRAF inhibitors via activation of C-RAF, COT, or N-RAS in melanoma would be blocked and tumor growth would theoretically be slowed or suppressed altogether. Indeed, MEK inhibitors have been shown to provide increased survival benefit in patients with BRAF or N-RAS-mutant melanoma both as a single agent or in combination with BRAF inhibition in initial clinical trials (11, 13, 26–30). In this study, *in vitro* and *in vivo* characterization of TAK-733 was carried out in preclinical models of malignant melanoma, including pharmacodynamic analyses. In addition, the antitumor activity of TAK-733 was assessed using patient-derived human tumor explant (PDTX) melanoma xenograft models. Finally, acquired resistance to TAK-733 was induced in a PDTX model by chronic administration of TAK-733. Gene expression analysis and gene set enrichment analyses were performed to identify potential mechanisms of resistance to this inhibitor *in vivo*.

Materials and Methods

Reagents and cell lines

TAK-733 (Supplementary Fig. S1) was provided by Takeda Cambridge US, Inc. under a materials transfer agreement and prepared as a 10-mmol/L stock solution in DMSO. For *in vivo* studies, this compound was prepared as a suspension in 0.5% methylcellulose in sterile water by brief vortexing followed by sonication for 10 minutes. The cutaneous melanoma cell lines were obtained from the ATCC and were cultured according to their recommendations. All cell lines except SK-MEL24 and Hs852t were maintained in DMEM supplemented with 10% FBS, 1% nonessential amino acids, 1% penicillin/streptomycin (Invitrogen), and were maintained at 37°C under an atmosphere of 95% O₂, 5% CO₂. SK-MEL 24 required 15% FBS and Hs852t required a 10% CO₂ atmosphere. Authenticity of all cell lines was verified by the University of Colorado Cancer Center DNA Sequencing (Aurora, CO) and Analysis Core using the Profiler Plus Kit (Applied Biosystems). The data obtained were compared with ATCC data to ensure that the cell line profiles had not changed with the latest profiling performed in January and February 2013.

Cell proliferation assays

The effects of TAK-733 on cell proliferation were determined using the sulforhodamine B (SRB) method (31). Briefly, cells in logarithmic growth phase were transferred to 96-well flat bottom plates with lids. Of note, 100 μ L cell suspensions containing 2,000 to 3,000 viable cells were plated into each well and incubated

overnight before exposure with increasing concentrations of TAK-733 for 72 hours. Postdrug administration, media were removed and cells were fixed with cold 10% trichloroacetic acid for 30 minutes at 4°C. Cells were then washed with water and stained with 0.4% SRB (Fisher Scientific) for 30 minutes at room temperature, washed again with 1% acetic acid, followed by stain solubilization with 10 mmol/L tris at room temperature. The absorbance at 565 nm was measured on a plate reader (Biotek Synergy 2). Cell proliferation curves were derived from the raw absorbance (OD) data. Statistical analyses and graphical representation of data were obtained using GraphPad Prism version 5.00 (GraphPad Software).

Immunoblotting

For *in vitro* studies, cell lines were seeded into 6-well plates and allowed to grow in complete media without drug for 24 hours. Cells were then switched to FBS-free media for 24 hours. On day 3, cells were exposed to DMSO or TAK-733 (0.125 μ mol/L) in FBS-free media for one hour, with and without addition of 10% FBS, was added to each well for 30 minutes. The cells were then scraped into RIPA buffer containing protease inhibitors, EDTA, sodium fluoride (NaF), and sodium orthovanadate. Total protein levels in samples were determined using the Bio-Rad DC Protein Assay (Bio-Rad). Thirty micrograms of total protein were loaded onto a 8% to 12% gradient gel, electrophoresed, and then transferred to PVDF using the I-Blot system (Invitrogen). The membranes were blocked for 1 hour at room temperature (RT) with 5% nonfat dry milk in TBS containing tween-20 (0.1%) before overnight incubation at 4°C with the following primary antibodies (clone): Cell Signaling Technology; pAKT (D9E), AKT (40D4), pERK (D13.14.4E), ERK (L34F12), pS6RP (D57.2.2E), S6RP (54D2), pPI3K (poly), PI3K (19H8), pBAD (40A9), caspase-3 (8G10), cleaved caspase-3 (5A1E), α -tubulin (DM1A), and β -actin (13E5). After primary antibody, blots were washed three times 20 minutes in TBS-Tween (0.1%), incubated with the appropriate secondary anti-rabbit or anti-mouse IgG infrared-linked antibody at 1:20,000 for 1 hour at RT, washed three times, and developed using the Licor Odyssey (Licor Inc).

NRAS and BRAF mutation analyses

For both melanoma cell lines and human tumor explants, DNA was isolated using the Qiagen DNA extraction kit (Qiagen). BRAF and NRAS mutations were analyzed by PCR amplification and direct sequencing of the products. The following PCR primers used: BRAF forward primer 5'-AACA-CATTCAAGCCCCAAA-3'; BRAF reverse primer 5'-GAAACTG-GTTTCAAAATATTCGGT-3'; NRAS forward primer 5'-CAGGAT-TCTTACAGAAAACAAGTGG-3'; NRAS reverse primer AACC-TAAACCAACTCTTCCCA-3'.

PD and PK sample collection and handling

Mice bearing A375 human melanoma xenografts were dosed by oral gavage. Animals were sacrificed using carbon dioxide at various time points following administration. Plasma was separated and frozen on dry ice, then stored at –80°C before being transferred for analysis. Subcutaneous tumors were removed from mice and divided into two parts. Both halves of each tumor were frozen on dry ice and stored at –80°C before determination of compound concentration or analyzed for pERK pharmacodynamic (PD) response.

For PD assessment, excised tumors were homogenized in an SDS-based lysis buffer using a BeadBeater (BioSpec Products). Lysates were spun at 2,000 rpm for 5 minutes at 4°C. Of note, 700 μ L was transferred to new tubes and spun at 12,000 rpm for 10 minutes at 4°C. Supernatants were transferred to 96-deepwell blocks, and protein concentrations were determined using a microBCA Assay (Pierce Biotechnology). Each sample was normalized to 3.0 mg/mL of total protein in 62.4 mmol/L Tris-HCl, pH 6.8, 2% SDS, 1% glycerol, 10% and 2% bromophenyl blue solution. Proteins were separated by electrophoresis using NuPage Bis-Tris gels (4%–12%) using 2-(N-morpholine) ethanesulfonic acid buffer, and transferred to polyvinylidene difluoride membranes (Millipore). Anti-pERK-1/2 (Thr202/Tyr204) and anti-total ERK-1/2 rabbit polyclonal (Cell Signaling Technology) were incubated overnight at 4°C to detect pERK-1/2 and anti-total ERK-1/2 proteins in the A375 xenograft model. Images of blots were collected on an Odyssey infrared imaging system (Li-Cor Biosciences) and signals corresponding to pERK and total ERK were quantified using Li-Cor software.

Quantitation of TAK-733

Compound concentrations in plasma were determined after precipitation of proteins in acetonitrile (Fisher Scientific). Tumor samples were homogenized in 5 volumes of water (i.e., 1 g tumor:4 mL water) using an Omni-prep homogenizer (Omni International). Samples were vortexed and then centrifuged at 3,000 rpm for 5 minutes at 4°C in a bench top Beckman Coulter Allegra 25R Centrifuge (Beckman Coulter). One hundred microliters of supernatant were transferred to 1.5 mL 96-well plate and dried down under a steady stream of nitrogen. Samples were reconstituted with 300 μ L of mobile phase (20:80 acetonitrile: water). Processed plasma samples were loaded by a Leap CTC PAL (Leap Technologies) autosampler onto a 2.5- μ m Synergi Polar-RP 100A, 2.0-mm internal diameter, 50-mm high-performance liquid chromatography column (Phenomenex, Inc.) and separated by gradient elution using a mixture of acetonitrile and water each containing 0.04% formic acid with the mobile phase at a flow rate of 0.5 mL/minute. The amount of acetonitrile in the mobile phase was 45%, at which it was held for 0.2 minutes from the beginning of the run. This was increased linearly to 95% over 0.7 minutes, and then increased linearly to 100% over 0.1 minutes and held at 90% until 1.6 minutes, whereupon it was decreased back to 45%. The run time was approximately 3.5 minutes. A PerkinElmer Sciex API 4000 LC/MS–MS system with an atmospheric pressure chemical ionization interface (Perkin-Elmer, Inc.) was used for detection. Multiple-reaction monitoring with dwell times of 100 and 80 msec was used to detect positive ions resulting from the mass-to-charge ratio (m/z) 504.96→431.00 transitions for TAK-733 and the m/z 509.09→435.00 transition for the SYR154628Z (internal standard), respectively. Quantitation was based upon integrating peaks corresponding to elution of the drug and internal standard in the extracted product ion chromatograms. The LLOQ for plasma was 0.25 ng/mL and tumor samples was 1.25 ng/g.

In vivo xenograft studies

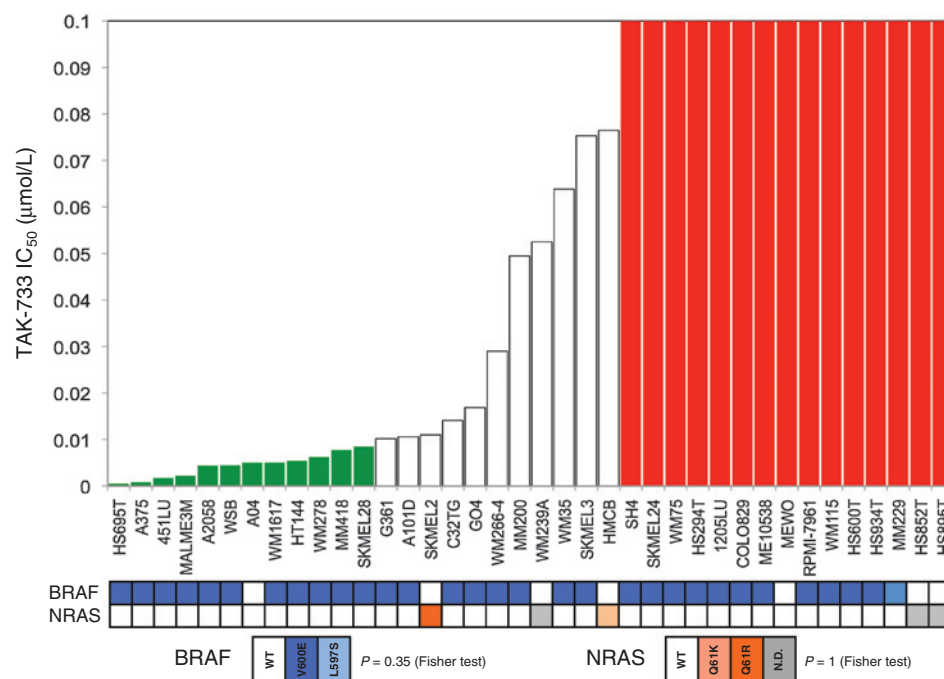
Five- to six-week-old female athymic nude mice (Harlan–Sprague–Dawley) were used. Mice were caged in groups of 5 and kept on a 12-hour light/dark cycle and provided with sterilized food and water *ad libitum*. Animals were allowed to acclimate for at least 7 days before any handling.

A375 human melanoma (ATCC) xenograft tumors were generated by harvesting cells from mid-log phase cultures using Trypsin-EDTA (Invitrogen, Inc.). Approximately 5×10^6 cells suspended in Hanks' balanced salt solution (GIBCO, Invitrogen Corp) were injected s.c. into the right flank of 6- to 8-week-old mice. Administration of TAK-733 was initiated when tumors in all mice in each experiment ranged in size from 100 to 200 mm³ for antitumor efficacy studies and from 300 to 500 mm³ for PD studies. All drug administrations were administered orally by gavage on the basis of group mean weight once daily for approximately 2 weeks. For administration, TAK-733 was formulated in a suspension of 0.5% methylcellulose 400 (Wako Chemical) in water.

Tumor growth was monitored at least twice weekly using vernier calipers, and tumor volume was calculated using the formula $(\text{length} \times \text{width}^2)/0.52$. Administrations producing >20% lethality and/or >20% net body weight loss were considered toxic. Antitumor effects were measured as the incidence of complete regressions (CR), partial regressions (PR), and tumor growth delay (TGD). CRs were defined as tumors that were no longer palpable. PRs were defined as tumors that were reduced by more than 50% but less than 100% of their initial size. A minimum duration of 7 days was required for a CR or PR to be considered durable. TGD was calculated by subtracting the time it takes (in days) for the median tumors in the untreated control groups to attain the evaluation size for that experiment from the time it takes for the median tumors in the treated group to reach the same size. Tumor growth inhibition (Treated/Control, %T/C) was calculated on the last day of administration. A negative T/C ratio indicated not only effective tumor growth inhibition in comparison with control, but also effective tumor volume reduction from day 1.

The PDX melanoma xenograft models were generated according to previously published methods (32). Briefly, surgical specimens of patients undergoing either removal of a primary melanoma or metastatic tumor at the University of Colorado Hospital were cut into 3 mm³ sections and implanted subcutaneously into 5 mice for each patient. Tumors were allowed to grow to a size of 1,000 to 1,500 mm³ (F1) at which point they were harvested, divided, and transplanted to another 5 mice (F2) to maintain the tumor bank. After a subsequent growth passage, tumors were excised and expanded into cohorts of mice for administration of TAK-733. All experiments were conducted on F3–F5 generations. Tumors from this cohort were allowed to grow until reaching approximately 150 to 300 mm³, at which time they were equally distributed by size into the two groups (vehicle control and TAK-733 administered). Mice were administered with either vehicle or TAK-733 (25 or 10 mg/kg) once daily by oral gavage. Mice were weighed twice weekly as a means of monitoring toxicity of TAK-733. Tumor size was evaluated three times per week by caliper measurements using the following formula: tumor volume = $(\text{length} \times \text{width}^2)/0.52$. Tumor volume and body weight data were collected using the Study Director software package (Studylog Systems). The tumor growth inhibition index was determined by calculating the tumor volume of TAK-733-administered mice at study end (T_{end}) minus volume of day 1 of administration (T_{start}) of administration divided by control at end of study (C_{end}) minus volume at day 1 (C_{start}). Tumors with a negative $(T_{\text{end}} - T_{\text{start}}/C_{\text{end}} - C_{\text{start}})$, which indicates regression, were considered sensitive. Those which showed statistically

Micel et al.

**Figure 1.**

Antiproliferative effects of TAK-733 against a panel of human cutaneous melanoma cell lines. Cell lines were treated with increasing doses of TAK-733 for 72 hours and proliferation was assessed using the SRB assay. IC₅₀ values are depicted. BRAF and NRAS mutational status is depicted in the table below.

significant growth inhibition compared with controls, but did not regress were considered intermediate responsiveness, and tumors that did not demonstrate significant growth inhibition compared with controls were considered resistant. All of the *in vivo* studies were conducted in accordance with the NIH guidelines for the care and use of laboratory animals was conducted in a facility accredited by the American Association for Accreditation of Laboratory Animal Care. The study protocol was approved by University of Colorado Institutional Animal Care and Use Committee before initiation. Tissue acquisition from consented melanoma patients at the time of removal of a primary tumor or biopsy was conducted under a Colorado Multi-Institutional Review Board-approved protocol.

Acquired TAK-733 resistance model

To develop acquired resistance to TAK-733 in a PDTX model, mice bearing the TAK-733-sensitive PDTX MB1374 on both flanks were administered QD with 100 mg/kg TAK-733 until visible outgrowth of individual tumors was observed. After approximately 2 months of administration, one flank tumor out of ten demonstrated outgrowth and was harvested when it reached a volume of approximately 300 mm³ (data not shown). Total RNA was extracted sequentially from: (i) tumor regrowth, (ii) readministration to sensitive, and (iii) administer to resistance tumors and gene expression was analyzed using Affymetrix Human 1.0 ST gene chips (accession number: GSE36133). Unsupervised hierarchical clustering was performed on these profiles and functional analysis of genes was performed using NIH DAVID (33).

Statistical analysis

To determine the statistical significance of BRAF mutational status and sensitivity to TAK-733, the Fisher exact test was performed using GraphPad Prism Software. Differences were considered significant at $P < 0.05$.

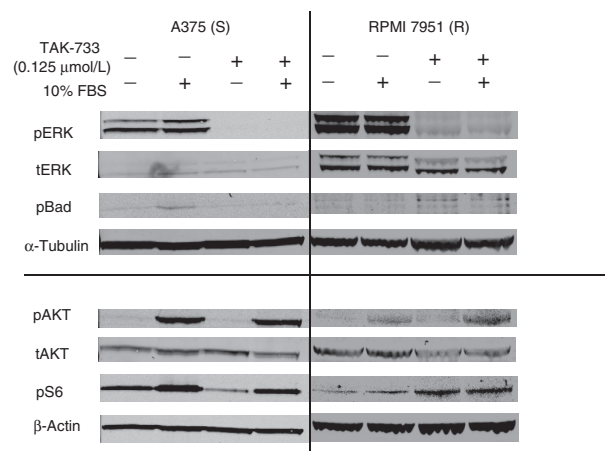
Results

In vitro antiproliferative effects of TAK-733 on melanoma cell lines

Thirty-four melanoma cell lines were exposed *in vitro* to increasing concentrations of TAK-733 for 72 hours. Of the 34 cell lines, 27 were BRAF^{V600E} mutant and seven were wild-type. SRB proliferation assays were performed and the resulting IC₅₀ concentrations allowed stratification of cell lines into three categories: relatively resistant, intermediate, and highly sensitive. Relatively resistant and highly sensitive lines were assigned on the basis of an IC₅₀ that differed by at least 10-fold (Fig. 1). Of note, there was no statistically significant association between BRAF status and response to TAK-733 *in vitro* ($P > 0.05$). Of note, these results were comparable with the approved MEK inhibitor trametinib in a subset of sensitive and resistant cell lines, whereas the activity of the approved BRAF inhibitor vemurafenib was much less potent (Supplementary Table S1).

Pharmacodynamic effects of TAK-733 on melanoma cell lines

To assess the impact of TAK-733 on downstream targets of the RAS/RAF/MEK pathway and to gain mechanistic insights into TAK-733 antitumor activity, immunoblotting studies were performed. One highly sensitive and three relatively resistant cell lines were exposed to TAK-733 for one hour and then harvested for isolation of total cellular protein. Immunoblotting of several canonical MEK pathway effectors and alternative effectors was analyzed and notably, the level of active, phosphorylated ERK (pERK) was downregulated in both the sensitive, A375 and resistant RPMI-7951, MeWo, and HS294T cell lines (Fig. 2 and Supplementary Fig. S2). Interestingly, in the HS294T cell line, TAK-733 administration preferentially affected p44 pERK levels, and to a lesser extent, p42 pERK (Supplementary Fig. S2). Although the mechanism for this selective inhibition remains unclear, it may indicate one potential factor in resistance to TAK-733 in this cell line. Interestingly, there was increased

**Figure 2.**

Immunoblot analysis of downstream effectors upon administration of TAK-733. A375 and RPMI-7951 cell lines were serum starved overnight and then administered TAK-733 for 1 hour. Cells were then challenged with 10% FBS for 30 minutes, harvested, and immunoblotted with the indicated antibodies.

expression of pAkt observed in both sensitive A375 and resistant HS294T and RPMI-7951 cells that was not suppressed by TAK-733 in the absence or presence of FBS. Similar studies were performed in complete media and longer TAK-733 administration time of 24 hours to assess apoptotic markers. As shown in Supplementary Fig. S3, TAK-733 failed to induce cleaved caspase-3 or pBAD expression under these conditions *in vitro*.

Pharmacokinetic/pharmacodynamic relationship of TAK-733 *in vivo*

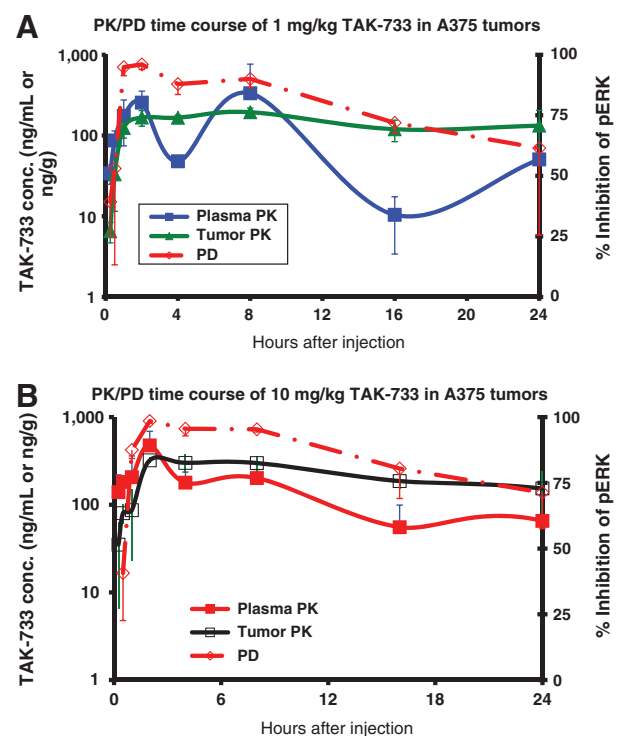
To assess PK/PD relationships, TAK-733 concentrations in plasma and tumor over time were quantitated in the sensitive A375 tumor-bearing mice. These data were then compared with the inhibition of tumor ERK phosphorylation over time as described in Materials and Methods (Fig. 3). Following an oral dose of 1 mg/kg, TAK-733 concentrations peaked rapidly and corresponded with a rapid reduction in pERK. Peak mean inhibition of pERK (>95%) was observed at 2 hours postdose and was associated with peak plasma (250 ng/mL) and tumor (170 ng/g) concentrations (Fig. 3A). Similar results were observed at a dose of 10 mg/kg (Fig. 3B). Tumor concentrations of TAK-733 remained elevated throughout the 24-hour time course and correlated with a mean inhibition of pERK of approximately 39% to 99% (Supplementary Table S2). The time course of pERK reduction corresponded approximately with the tumor concentrations, as depicted in Fig. 3A. Mean plasma concentration of TAK-733 decreased rapidly from 8 hours to 16 hours postdose. A summary of the 24 and 48 plasma and tumor concentrations of TAK-733 is presented in Supplementary Table S3.

Antitumor activity of TAK-733 in athymic nude mice bearing A375 human melanoma tumors

Daily oral administration of 1, 3, 10, and 30 mg/kg of TAK-733 for 14 days (days 10–23) resulted in tumor growth delay in the A375 cell-implanted mice (5/group; Fig. 4 and Supplementary Table S4). TAK-733 (35, 70, 100, and 160 mg/kg) also significantly inhibited tumor growth on an intermittent dosing schedule of 3 days per week for 2 weeks (days 10, 13, 15, 17, 20, and 22). Three PRs, a 60% response rate, were observed in mice administered with 30 mg/kg of TAK-733 daily and in mice adminis-

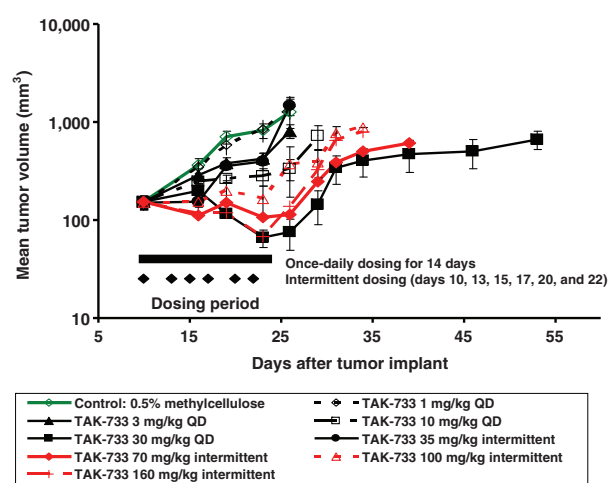
tered with 160 mg/kg of TAK-733 intermittently. Responses, CR, and PR were also observed in mice administered with 70, 100, and 160 mg/kg of TAK-733 intermittently. The tumor regression rate was more pronounced with the intermittent administration regimen; the greatest reduction in tumor volume was observed at 160 mg/kg (57.29%), versus a maximum reduction of 46.97% at 30 mg/kg once daily (Supplementary Table S4). By the last day of administration, tumor growth was significantly ($P < 0.05$ for %T/C, Student *t* test) inhibited in mice administered 3, 10, and 30 mg/kg once daily or 35, 70, 100, and 160 mg/kg intermittently.

To assess the potential effects of TAK-733 against human melanoma tumors, PDTX models were established in athymic nude mice. Because they are never cultured on plastic, PDTX models recapitulate the human tumor from which they were derived with respect to tumor architecture, stroma, mutational status, etc. and are thus considered more stringent models for efficacy studies (32, 34). The nude mice carrying the PDTX were then randomized into two groups: control and TAK-733 administered (10 or 25 mg/kg) once daily by oral gavage as described in Materials and Methods, and tumors were measured by caliper three times per week. Figure 5A depicts the percent change in volume from baseline in administered tumors measured at the end of study. A total of eleven individual PDTXs were administered with TAK-733. Of these, six harbored the BRAF^{V600E} mutation, five were BRAF^{WT}, one model carried an NRAS^{Q61L} mutation, and one model carried an NRAS^{Q61H} mutation. Amongst these

**Figure 3.**

Pharmacokinetic and pharmacodynamic effects of TAK-733 in A375 tumor-bearing mice following oral administration of 1 mg/kg (A) or 10 mg/kg (B) dose. A375 tumor cells were implanted subcutaneously in the flank of nu/nu mice (3/time point). Administration was initiated when all mice had tumors ranging in size from 300 to 500 mm³ (day 10). TAK-733 was given as a single oral dose. Tumor pERK levels were monitored by immunoblot analysis using phospho-specific antibodies.

Micel et al.

**Figure 4.**

Effects of TAK-733 on growth of A375 melanoma tumor xenografts in athymic nude mice. A375 melanoma cells were implanted subcutaneously in the flank of nu/nu mice (5/group). Administration was initiated 10 days after the tumor implant, when all mice had tumors ranging in size from 80 to 225 mm³ (day 10). TAK-733 was given orally daily for 14 days (QD 1-14) or 3 days per week for two cycles (M, TH, SAT × 2).

models, BRAF and NRAS mutations were mutually exclusive. In all but one PDTX, MB947 (BRAF^{V600E}, $P = 0.41$), TAK-733 demonstrated statistically significant antitumor activity when compared with controls ($P < 0.0001$ – 0.03). Furthermore, in 45% of the mice administered with TAK-733, tumor regression was observed. Representative growth curves are depicted in Fig. 5B–E. Somewhat surprisingly, there was no association between BRAF^{V600E} mutational status and responsiveness to TAK-733 in these PDTX models ($P > 0.5$). A representative PDTX model, MB 1255, is depicted in Supplementary Fig. S4, demonstrating increased antitumor activity.

To assess tumor regrowth kinetics after administration of TAK-733, administration was discontinued in one model, MB1374, and tumor regrowth was observed after approximately 60 days. Dosing with TAK-733 was then restarted 111 days after the prior cessation and tumor regression was again observed (Fig. 6). A similar pattern of tumor growth and regression was observed after a second TAK-733 holiday followed by the reinstitution of dosing.

The doses and schedule used in this study (10 and 25mg/kg/day) were within the tolerability limits for TAK-733 in mice and no animals exhibited obvious signs of toxicity as indicated by outward morbidity or weight loss. Tumor samples harvested at the end of the study were collected 1 hour after TAK-733 administration and evaluated for pharmacodynamic response. As depicted in Supplementary Fig. S5, pERK was downregulated in the TAK-733 administered mice compared with controls, regardless of BRAF^{V600E} mutational status, confirming inhibition of MEK by TAK-733. Interestingly, pS6 protein, a downstream substrate of P-70 S6 kinase and an effector of the PI3K pathway, was robustly inhibited (particularly taking into account the loading control of α -tubulin) in the resistant MB947 PDTX, which was also observed in MB1547 but not MB1337.

Acquired resistance to TAK-733 in PDTX model

Acquired resistance to TAK-733 was observed as outgrowth of a single MB1374 tumor administered chronically with

25 mg/kg TAK-733 for 2 months (data not shown). To examine genetic alterations associated with the acquired resistance to TAK-733, samples from tumor regrowth, readminister to sensitive and administer to resistance from the sensitive explant model MB1374 (Fig. 6) were harvested. Global gene expression profiling identified transcriptional changes after acquired resistance to TAK-733. Unsupervised hierarchical clustering on these profiles demonstrated that the tumor regrowth and administer to resistance samples clustered together, suggesting that there are similar transcriptional profiles and differences from the readminister to sensitive profile (Supplementary Fig. S6). Using gene expression changes of 1.5-fold change as cutoff, we identified that 289 and 133 genes were up- and downregulated in the two resistant samples as compared with the readminister to sensitive. Functional analysis of these genes by NIH DAVID (33) revealed that the upregulated genes in the resistant samples were enriched with cell adhesion molecules ($P = 8.7 \times 10^{-5}$, FDR = 0.009) and axon guidance ($P = 0.009$, FDR = 0.09), whereas downregulated genes were involved in homologous recombination ($P = 0.002$, FDR = 0.02) and systemic lupus erythematosus ($P = 0.01$, FDR = 0.1), according to KEGG pathway definitions (35).

Discussion

Although the significance of the discovery of the BRAF^{V600E/K} mutation and its role as a driver mutation in the development and progression of malignant melanoma has been substantial, the clinical translation of this discovery into effective therapeutics has been relatively short-lived due to *de novo* or acquired resistance (11, 22, 23). Viable alternative therapies for this patient population include the recently approved use of MEK inhibitors either as single agents or in combination with RAF inhibitors (17, 27, 28). However, the clinical efficacy of MEK inhibitors tested to date has been modest, likely due to a narrow therapeutic window, highlighting the need for the development of more potent compounds with improved toxicity profiles. The goal of this study was to evaluate the activity of a potent and selective MEK inhibitor, TAK-733, against preclinical models of melanoma. Although previous studies have been conducted demonstrating TAK-733 activity against melanoma cell lines *in vitro* (25), we sought to expand these studies into more clinically relevant *in vivo* murine models of melanoma. The translation of preclinical evidence into clinical practice success has historically been challenging and often fruitless. A number of factors, including genetic changes and divergence in cell lines grown outside the normal tumor environment, genetic divergence between the primary tumor and corresponding cell line, and heterogeneous patient tumors, are cited as likely culprits for the lack of successful preclinical to clinical translation (34, 36). The use of PDTX is increasingly being applied in oncology drug development as these models retain the molecular and genetic heterogeneity of human tumors and thus provide a more clinically relevant model for analysis of drug activity and predictive biomarker development (32, 34, 37, 38). Here, we utilized 11 distinct PDTX models, representing varying genetic backgrounds to assess the antitumor activity of TAK-733.

Preclinical and clinical studies have demonstrated that tumors harboring BRAF^{V600} mutations confer an oncogene addiction to the MAPK pathway for survival, providing an opportunity for therapeutic intervention (11, 14, 29, 39–43). Although targeting BRAF is a logical and effective therapeutic strategy, these tumors

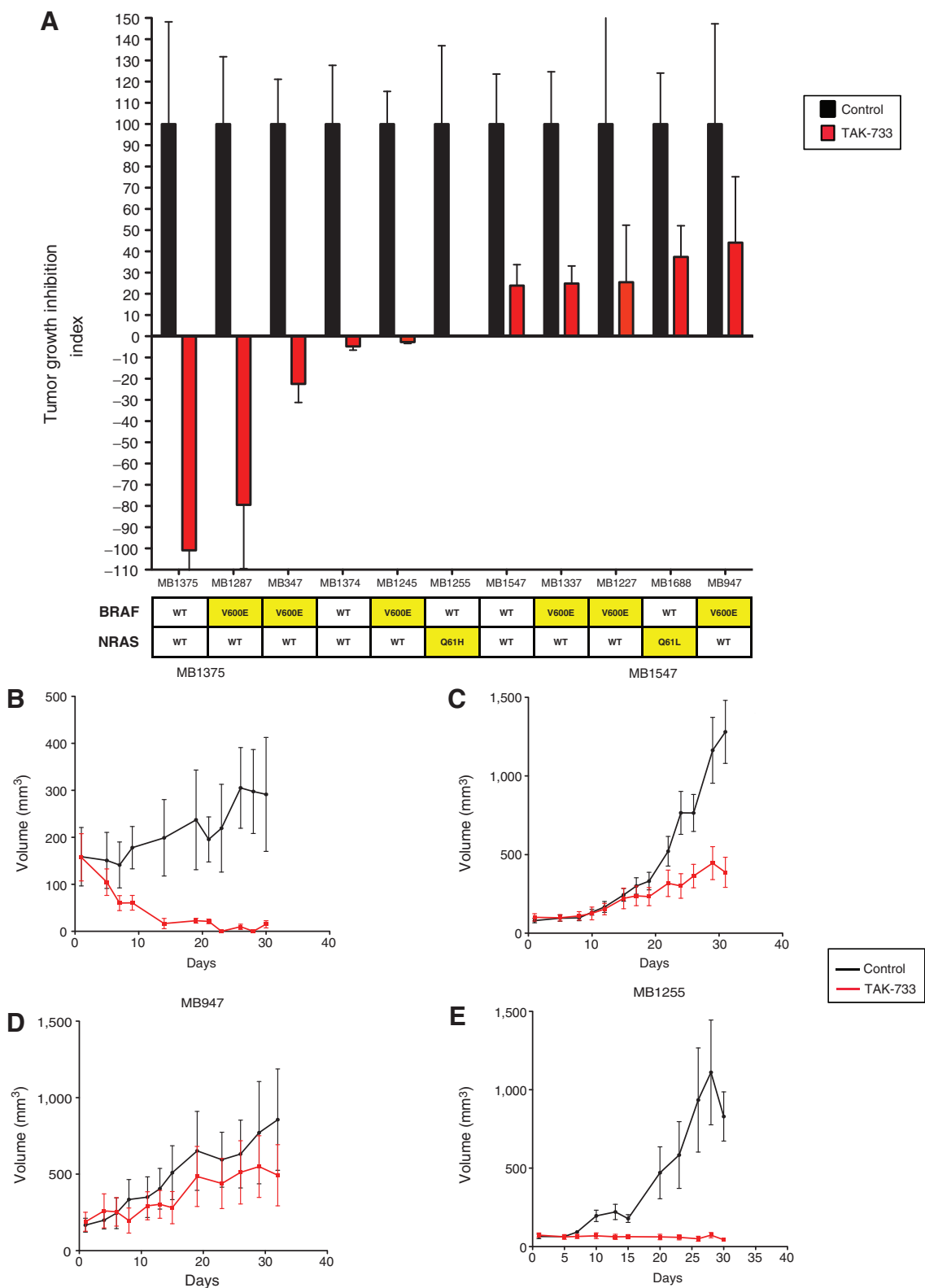


Figure 5. A, tumor growth inhibition index of 11 PDTC tumor models administered with TAK-733 (10 mg/kg) for 30 days. B–E, representative tumor growth inhibition curves of four melanoma PDTC models administered with vehicle or TAK-733 (10 mg/kg) for the indicated study days.

Micel et al.

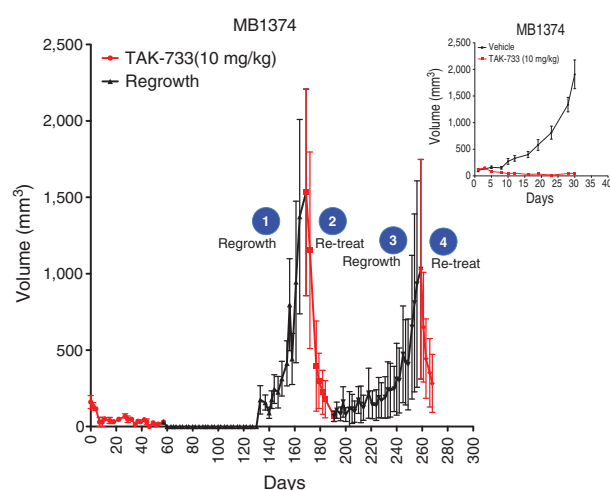


Figure 6. Tumor regrowth kinetics for PDTX model MB1374 administered with vehicle or TAK-733 (10 mg/kg). Inset, original tumor growth inhibition study for 30 days. Red lines indicate TAK-733 administration times and black lines indicate cessation of TAK-733 for tumor regrowth periods.

inevitably acquire additional mutations that allow them to bypass the inhibition, resulting in relapse and tumor progression. The types of resistance identified to date include MAPK pathway-dependent mechanisms such as upregulation of NRAS and subsequent signaling through CRAF (21, 22), upregulation of the MAP3K8 gene COT, which can drive MAPK signaling through MEK-dependent mechanisms independent of RAF signaling (20), and activating mutations in MEK (19, 23). These findings have directed the design of clinical trials testing the rational combination of BRAF^{V600} and MEK inhibitors which have resulted in improved survival in patients with BRAF^{V600}-mutant melanoma compared with BRAF inhibitors alone, highlighting the need for effective MEK inhibitors (28). In addition, MAPK-independent resistance mechanisms have been identified, including upregulation of receptor tyrosine kinases such as PDGFR α that may signal through the PI3K/AKT pathway (22) and dictate novel combination strategies targeting these pathways.

The activity of TAK-733 observed in both BRAF^{WT} and BRAF^{V600E} melanoma models suggests that it may have distinct therapeutic potential. Two of the TAK-733-responsive BRAF^{WT} PDTX models harbored NRAS mutations, supporting the notion that MEK1/2 inhibition may be an effective therapeutic target for BRAF^{WT} patients carrying an alternate driver mutation in the MAPK pathway. The association of additional driver mutations and responsiveness to TAK-733 deserves further study that could provide the rationale for treatment of a defined molecular subset of BRAF^{WT} patients.

In this study, we observed antitumor activity of TAK-733 against PDTX melanoma models. Indeed, of the 11 PDTX tested, we found only one example of a resistant model, MB947, which is a V600E mutant. The level of activity and lack of resistance observed in 91% of our explant models suggest that resistance to BRAF inhibitors conferred through activating mutations in MEK can potentially be overcome by a potent MEK inhibitor, such as TAK-733. Interestingly, immunoblotting demonstrated pERK downregulation in the resistant MB947 tumors suggesting effective MEK inhibition that may be necessary but not sufficient for antitumor activity. Cross-talk between the MAPK and

PI3K/AKT pathways represents a potential bypass to MEK inhibition; however, upregulation of the PI3K/AKT pathway was not consistently observed. These findings suggest alternative resistance mechanisms outside of the MAPK pathway that have yet to be identified. Despite the activity of TAK-733 in these PDTX models, we expect that similar to other targeted therapies, resistance is likely to develop.

To identify potential mechanisms of acquired resistance to TAK-733, we administered a sensitive PDTX model with TAK-733 to resistance, as measured by escape from tumor growth inhibition. Unbiased gene expression analysis identified genes and pathways that were differentially expressed between tumor regrowth, readministration to sensitive, and administration to resistance samples from the sensitive explant model MB1374. Among the core genes of the axon guidance are EPHA2, EPHB4, ABLIM3, SEMA3D, L1CAM, SEMA3A, and NFATC2. Notably, overexpression of EPHA2 (EPH receptor A2) has been identified as a resistance mechanism to HER2 treatment in breast cancer (44), suggesting cross-talk between EphA and the RAS/RAF/MEK signaling pathway in the resistance stage (45).

In summary, TAK-733 demonstrated potent antitumor activity *in vitro* and *in vivo* in preclinical melanoma models of melanoma. Tumor regression was observed in 45% of murine PDTX models which is remarkable and suggests that further studies in humans are warranted. On the basis of the recently characterized resistance mechanisms of targeted BRAF inhibitors in patients with melanoma, the combination of TAK-733 with other agents such as BRAF or PI3K pathway inhibitors could potentially exhibit synergistic effects and may lead to more durable clinical benefit in subsequent studies.

Disclosure of Potential Conflicts of Interest

S.G. Eckhardt reports receiving a commercial research grant from and is a consultant/advisory board member for Takeda Inc. No potential conflicts of interest were disclosed by the other authors.

Authors' Contributions

Conception and design: L.N. Micel, J.J. Tentler, A.-C. Tan, T.M. Pitts, E. Gangolli, P.W. Vincent, S.G. Eckhardt

Development of methodology: L.N. Micel, J.J. Tentler, A.-C. Tan, T.M. Pitts, P.W. Vincent, S.G. Eckhardt

Acquisition of data (provided animals, acquired and managed patients, provided facilities, etc.): L.N. Micel, J.J. Tentler, A.-C. Tan, H.M. Selby, K.L. Brunkow, K.M. Robertson, S.L. Davis, P.J. Klauck, T.M. Pitts, R. Fabrey, S.M. O'Connell, P.W. Vincent, S.G. Eckhardt

Analysis and interpretation of data (e.g., statistical analysis, biostatistics, computational analysis): L.N. Micel, J.J. Tentler, A.-C. Tan, H.M. Selby, K.L. Brunkow, K.M. Robertson, T.M. Pitts, R. Fabrey, P.W. Vincent, S.G. Eckhardt

Writing, review, and/or revision of the manuscript: L.N. Micel, J.J. Tentler, A.-C. Tan, P.J. Klauck, E. Gangolli, P.W. Vincent, S.G. Eckhardt

Administrative, technical, or material support (i.e., reporting or organizing data, constructing databases): K.L. Brunkow, K.M. Robertson, P.J. Klauck, T.M. Pitts

Study supervision: J.J. Tentler, T.M. Pitts, E. Gangolli, S.G. Eckhardt

Grant Support

This work was supported by NIH P30CA046934 (to S.G. Eckhardt and J.J. Tentler).

The costs of publication of this article were defrayed in part by the payment of page charges. This article must therefore be hereby marked *advertisement* in accordance with 18 U.S.C. Section 1734 solely to indicate this fact.

Received November 27, 2013; revised October 20, 2014; accepted October 23, 2014; published OnlineFirst November 5, 2014.

References

1. Siegel R, Naishadham D, Jemal A. Cancer statistics, 2012. *CA Cancer J Clin* 2012;62:10–29.
2. Boutros T, Chevet E, Metrakos P. Mitogen-activated protein (MAP) kinase/ MAP kinase phosphatase regulation: roles in cell growth, death, and cancer. *Pharmacol Rev* 2008;60:261–310.
3. Dhillion AS, Hagan S, Rath O, Kolch W. MAP kinase signaling pathways in cancer. *Oncogene* 2007;26:3279–90.
4. McCubrey JA, Steelman LS, Chappell WH, Abrams SL, Wong EW, Chang F, et al. Roles of the Raf/MEK/ERK pathway in cell growth, malignant transformation and drug resistance. *Biochim Biophys Acta* 2007;1773:1263–84.
5. Reddy KB, Nabha SM, Atanaskova N. Role of MAP kinase in tumor progression and invasion. *Cancer Metastasis Rev* 2003;22:395–403.
6. Davies H, Bignell GR, Cox C, Stephens P, Edkins S, Clegg S, et al. Mutations of the BRAF gene in human cancer. *Nature* 2002;417:949–54.
7. Kim EK, Choi EJ. Pathological roles of MAPK signaling pathways in human diseases. *Biochim Biophys Acta* 2010;1802:396–405.
8. Steelman LS, Abrams SL, Shelton JG, Chappell WH, Basecke J, Stivala F, et al. Dominant roles of the Raf/MEK/ERK pathway in cell cycle progression, prevention of apoptosis and sensitivity to chemotherapeutic drugs. *Cell Cycle* 2010;9:1629–38.
9. Hocker T, Tsao H. Ultraviolet radiation and melanoma: a systematic review and analysis of reported sequence variants. *Hum Mutat* 2007;28:578–88.
10. Hatzivassiliou G, Song K, Yen I, Brandhuber BJ, Anderson DJ, Alvarado R, et al. RAF inhibitors prime wild-type RAF to activate the MAPK pathway and enhance growth. *Nature* 2010;464:431–5.
11. Flaherty KT, Puzanov I, Kim KB, Ribas A, McArthur GA, Sosman JA, et al. Inhibition of mutated, activated BRAF in metastatic melanoma. *N Engl J Med* 2010;363:809–19.
12. Joseph EW, Pratilas CA, Poulikakos PI, Tadi M, Wang W, Taylor BS, et al. The RAF inhibitor PLX4032 inhibits ERK signaling and tumor cell proliferation in a V600E BRAF-selective manner. *Proc Natl Acad Sci U S A* 2010;107:14903–8.
13. Ribas A, Flaherty KT. BRAF targeted therapy changes the treatment paradigm in melanoma. *Nat Rev Clin Oncol* 2011;8:426–33.
14. Solit DB, Garraway LA, Pratilas CA, Sawai A, Getz G, Basso A, et al. BRAF mutation predicts sensitivity to MEK inhibition. *Nature* 2006;439:358–62.
15. Chapman MS, Miner JN. Novel mitogen-activated protein kinase kinase inhibitors. *Expert Opin Investig Drugs* 2011;20:209–20.
16. McCubrey JA, Steelman LS, Abrams SL, Chappell WH, Russo S, Ove R, et al. Emerging MEK inhibitors. *Expert Opin Emerg Drugs* 2010;15:203–23.
17. Sebolt-Leopold JS. MEK inhibitors: a therapeutic approach to targeting the Ras-MAP kinase pathway in tumors. *Curr Pharm Des* 2004;10:1907–14.
18. Wang D, Boerner SA, Winkler JD, LoRusso PM. Clinical experience of MEK inhibitors in cancer therapy. *Biochim Biophys Acta* 2007;1773:1248–55.
19. Emery CM, Vijayendran KG, Zipser MC, Sawyer AM, Niu L, Kim JJ, et al. MEK1 mutations confer resistance to MEK and B-RAF inhibition. *Proc Natl Acad Sci U S A* 2009;106:20411–6.
20. Johannessen CM, Boehm JS, Kim SY, Thomas SR, Wardwell L, Johnson LA, et al. COT drives resistance to RAF inhibition through MAP kinase pathway reactivation. *Nature* 2010;468:968–72.
21. Montagut C, Sharma SV, Shioda T, McDermott U, Ullman M, Ullkus LE, et al. Elevated CRAF as a potential mechanism of acquired resistance to BRAF inhibition in melanoma. *Cancer Res* 2008;68:4853–61.
22. Nazarian R, Shi H, Wang Q, Kong X, Koya RC, Lee H, et al. Melanomas acquire resistance to B-RAF(V600E) inhibition by RTK or N-RAS upregulation. *Nature* 2010;468:973–7.
23. Wagle N, Emery C, Berger MF, Davis MJ, Sawyer A, Pochanard P, et al. Dissecting therapeutic resistance to RAF inhibition in melanoma by tumor genomic profiling. *J Clin Oncol* 2011;29:3085–96.
24. Dong Q, Dougan DR, Gong X, Halkowycz P, Jin B, Kanouni T, et al. Discovery of TAK-733, a potent and selective MEK allosteric site inhibitor for the treatment of cancer. *Bioorg Med Chem Lett* 2011;21:1315–9.
25. von Euw E, Atefi M, Attar N, Chu C, Zachariah S, Burgess BL, et al. Antitumor effects of the investigational selective MEK inhibitor TAK733 against cutaneous and uveal melanoma cell lines. *Mol Cancer* 2012;11:22–5.
26. Chapman PB, Hauschild A, Robert C, Haanen JB, Ascierto P, Larkin J, et al. Improved survival with vemurafenib in melanoma with BRAF V600E mutation. *N Engl J Med* 2011;364:2507–16.
27. Flaherty KT, Infante JR, Daud A, Gonzalez R, Keefe RF, Sosman J, et al. Combined BRAF and MEK Inhibition in Melanoma with BRAF V600 Mutations. *N Engl J Med* 2012;367:1694–703.
28. Flaherty KT, Robert C, Hersey P, Nathan P, Garbe C, Milhem M, et al. Improved survival with MEK inhibition in BRAF-mutated melanoma. *N Engl J Med* 2012;367:107–14.
29. Infante JR. Safety and efficacy results from the first-in-human study of the oral MEK 1/2 inhibitor, GSK1120212. *J Clin Oncol* 28:15s, 2010 (suppl; abstr 2503).
30. Sosman JA, Kim KB, Schuchter L, Gonzalez R, Pavlick AC, Weber JS, et al. Survival in BRAF V600-mutant advanced melanoma treated with vemurafenib. *N Engl J Med* 2012;366:707–14.
31. Skehan P, Storeng R, Scudiero D, Monks A, McMahon J, Vistica D, et al. New colorimetric cytotoxicity assay for anticancer-drug screening. *J Natl Cancer Inst* 1990;82:1107–12.
32. Rubio-Viqueira B, Jimeno A, Cusatis G, Zhang X, Iacobuzio-Donahue C, Karikari C, et al. An *in vivo* platform for translational drug development in pancreatic cancer. *Clin Cancer Res* 2006;12:4652–61.
33. Huang da W, Sherman BT, Lempicki RA. Systematic and integrative analysis of large gene lists using DAVID bioinformatics resources. *Nat Protoc* 2009;4:44–57.
34. Tentler JJ, Tan AC, Weekes CD, Jimeno A, Leong S, Pitts TM, et al. Patient-derived tumor xenografts as models for oncology drug development. *Nat Rev Clin Oncol* 2012;9:338–50.
35. Kanehisa M, Goto S, Sato Y, Furumichi M, Tanabe M. KEGG for integration and interpretation of large-scale molecular data sets. *Nucleic Acids Res* 2012;40:D109–14.
36. Daniel VC, Marchionni L, Hierman JS, Rhodes JT, Devereux WL, Rudin CM, et al. A primary xenograft model of small-cell lung cancer reveals irreversible changes in gene expression imposed by culture *in vitro*. *Cancer Res* 2009;69:3364–73.
37. Pitts TM, Tan AC, Kulikowski GN, Tentler JJ, Brown AM, Flanagan SA, et al. Development of an integrated genomic classifier for a novel agent in colorectal cancer: approach to individualized therapy in early development. *Clin Cancer Res* 2010;16:3193–204.
38. Tentler JJ, Nallapareddy S, Tan AC, Spreafico A, Pitts TM, Morelli MP, et al. Identification of predictive markers of response to the MEK1/2 inhibitor selumetinib (AZD6244) in K-ras-mutated colorectal cancer. *Mol Cancer Ther* 2010;9:3351–62.
39. Hoefflich KP, Herter S, Tien J, Wong L, Berry L, Chan J, et al. Antitumor efficacy of the novel RAF inhibitor GDC-0879 is predicted by BRAFV600E mutational status and sustained extracellular signal-regulated kinase/mitogen-activated protein kinase pathway suppression. *Cancer Res* 2009;69:3042–51.
40. McDermott U, Sharma SV, Dowell L, Greninger P, Montagut C, Lamb J, et al. Identification of genotype-correlated sensitivity to selective kinase inhibitors by using high-throughput tumor cell line profiling. *Proc Natl Acad Sci U S A* 2007;104:19936–41.
41. Wan PT, Garnett MJ, Roe SM, Lee S, Niculescu-Duvaz D, Good VM, et al. Mechanism of activation of the RAF-ERK signaling pathway by oncogenic mutations of B-RAF. *Cell* 2004;116:855–67.
42. Wellbrock C, Ogilvie L, Hedley D, Karasarides M, Martin J, Niculescu-Duvaz D, et al. V599EB-RAF is an oncogene in melanocytes. *Cancer Res* 2004;64:2338–42.
43. Schwartz GK. A phase I study of XL281, a selective oral RAF kinase inhibitor, in patients with advanced solid tumors. *J Clin Oncol* 27:15s, 2009 (suppl; abstr 3513).
44. Zhuang G, Brantley-Sieders DM, Vaught D, Yu J, Xie L, Wells S, et al. Elevation of receptor tyrosine kinase EphA2 mediates resistance to trastuzumab therapy. *Cancer Res* 2010;70:299–308.
45. Miao H, Wei BR, Peehl DM, Li Q, Alexandrou T, Schelling JR, et al. Activation of EphA receptor tyrosine kinase inhibits the Ras/MAPK pathway. *Nat Cell Biol* 2001;3:527–30.

Molecular Cancer Therapeutics

Antitumor Activity of the MEK Inhibitor TAK-733 against Melanoma Cell Lines and Patient-Derived Tumor Explants

Lindsey N. Micel, John J. Tentler, Aik-Choon Tan, et al.

Mol Cancer Ther 2015;14:317-325. Published OnlineFirst November 5, 2014.

Updated version	Access the most recent version of this article at: doi: 10.1158/1535-7163.MCT-13-1012
Supplementary Material	Access the most recent supplemental material at: http://mct.aacrjournals.org/content/suppl/2014/11/04/1535-7163.MCT-13-1012.DC1.html

Cited Articles	This article cites by 43 articles, 14 of which you can access for free at: http://mct.aacrjournals.org/content/14/2/317.full.html#ref-list-1
-----------------------	---

E-mail alerts	Sign up to receive free email-alerts related to this article or journal.
Reprints and Subscriptions	To order reprints of this article or to subscribe to the journal, contact the AACR Publications Department at pubs@aacr.org .
Permissions	To request permission to re-use all or part of this article, contact the AACR Publications Department at permissions@aacr.org .